

Sand movement patterns in the Western Desert of Egypt: an environmental concern

Mohamed E. Hereher

Received: 5 November 2008 / Accepted: 9 February 2009 / Published online: 24 February 2009
© Springer-Verlag 2009

Abstract Wind action is the most dominant agent for erosion and deposition in the vast Western Desert of Egypt. Analysis of wind data from seven meteorological stations distributed along the Western Desert reveals that this desert is characterized by high-energy wind environments along the northern and southern edges and low-energy wind environments throughout the rest of the desert. Accordingly, sand drift potential follows the pattern of wind energy. Maximum sand drift potential was observed at the southern edge (571 vector units, which equals $40 \text{ m}^3/\text{m}$ width/year). Sand drift direction was observed towards the southeast except at the southern part of the desert where the trend of sand movement was towards southwest. The major dune type recognized on satellite images was the simple linear type. Linear dunes are generally associated with bimodal wind regime. Rates of sand drift potential and sand dune migration were greatest at East of Owinat region at the extreme southern part of the desert. Measurements of crescentic sand dune advance from two satellite images reveal a maximum advance rate of about 9 m/year at the southern part of the desert. Dune movement creates potential hazard to the infrastructures in this open desert.

Keywords Western Desert · Sand dunes · Drift potential · Landsat

Introduction

Egypt occupies an area of about $1.0 \times 10^6 \text{ km}^2$. Geomorphologically, Egypt consists of four different geomorphologic units, namely the Western Desert, the Eastern Desert, the Nile Valley and its delta, and Sinai Peninsula. The Western Desert of Egypt is the largest expanse of extreme aridity on the earth's surface (Goudie 2002). This desert, which occupies about 68% of the total area of Egypt, was the area where most important ideas and theories about sand dune formation and movement emerged. Bagnold (1941) deduced his hypotheses on the physics of blown sands from his observations of dune movement in Western Desert. Moreover, the physiography, geomorphology and landforms of this desert lead to some theories about the landforms of Mars (El-Baz and Maxwell 1982).

The Western Desert of Egypt is generally a plateau desert, where the exposed surface rocks include Cretaceous Nubian sandstone in the south; Cretaceous and Eocene limestone rocks in the central part; and Miocene limestone and calcareous sandstone rocks in the north (Gifford et al. 1979). This desert attains its highest peak at its southwest corner (Gebel Oweinat) and slopes gradually northward towards the Mediterranean Sea. It has an average elevation of 180 m above sea level. Its lowest point lies at Qattara Depression at the north with its base at 134 m below sea level. The surface of the Western Desert is covered by bare rocky plateaus, sandy sheets, fields of sand dunes and numerous closed-in to semi-closed depressions. Sand deposits cover about 27% of the total area of this desert (Gifford et al. 1979).

Most of the desert areas receive little precipitation because they occur in regions where there are subsiding air masses, and relative atmospheric constancy associated with the presence of high-pressure cells around altitude 30°

M. E. Hereher (✉)
Department of Environmental Sciences,
Faculty of Science at Damietta,
New Damietta City, Egypt
e-mail: mhereher@yahoo.com

(Goudie 2002). Rainfall in the Western Desert is very rare and occurs mainly from cyclonic winter storms, which could occur once every 10–20 years (Brookes 2003). The annual rainfall approaches 200 mm along the Mediterranean coast and decreases southward to about 30 mm at the latitude of Cairo. Moving southward, the annual rainfall becomes just a few millimetres near El-Kharga and El-Dakhla Oases at the south (Goudie 2002). Daily temperatures reach 42°C during summer with potential evapotranspiration rates of 14–15 mm/day (Vogg and Wehmeier 1985). However, this part of the Sahara Desert witnessed a number of dry–wet cycles during the Quaternary (Le Houerou 1997) and there is geographical, geological, and archaeological evidence of wetter climates in the past (El-Baz et al. 2000). Wind action is the dominant geomorphologic factor prevailing in this extremely arid region.

Several studies have attempted to provide an understanding of the aeolian dynamics and landforms in this desert. For example, Gifford et al. (1979) applied the orbital imagery of the Apollo-Soyuz Test Project photographs to delineate sand deposits. They observed that the dunes trend in a clockwise pattern, where they follow a north–northwesterly direction in the northern desert to north–northeasterly in the south. El-Baz (1986) studied the effect of topography on the alignment of sand dunes. He concluded that at El-Kharga and El-Farafra depressions, the sand dune orientation is controlled mainly by the direction of the depression scarp. Tag El-Din (1986) estimated the sand dune movement at El-Kharga and El-Dakhla Oases areas to be at 8–10 m per year. Embaby (1986) in his comparative study of dune movement at both El-Kharga and El-Dakhla Oases reported that the movement was higher in El-Kharga than in El-Dakhla and the trend of sand movement was mainly towards south. Abu El-Ennan et al. (1990) used Landsat satellite images to recognize sand accumulations at selected locations along the Western Desert, the Nile Valley and Sinai. They mentioned that longitudinal and linear dunes of the active type prevail at El-Kharga Oasis. El-Baz et al. (2000) and Ghoneim and El-Baz (2007) attributed the source of the sand in the Sahara Desert to the fluvial processes, which thereafter reworked and deposited elsewhere by wind in later dryer ages. Brookes (2003) concluded with the aid of Landsat MSS images that geomorphic aeolian indicators of Holocene wind directions indicate two main orientations: west and northwest and the other is from north and northeast.

Due to the occurrence of extreme drought conditions and lack of vegetation cover, the sand dunes are fully exposed and can be observed and distinguished clearly from the sky, giving the advantage to satellite remote sensing for an overall synoptic coverage. These dunes

create serious problems in the oases and new agricultural lands and settlements in the Western Desert. The main objectives of the present study are to study the sand drift potential in the Western Desert of Egypt based on surface wind data from specific meteorological station, to correlate the dune forms at each location with their wind regimes and to estimate the sand dune movement as measured from satellite data in specific locations.

Materials and methods

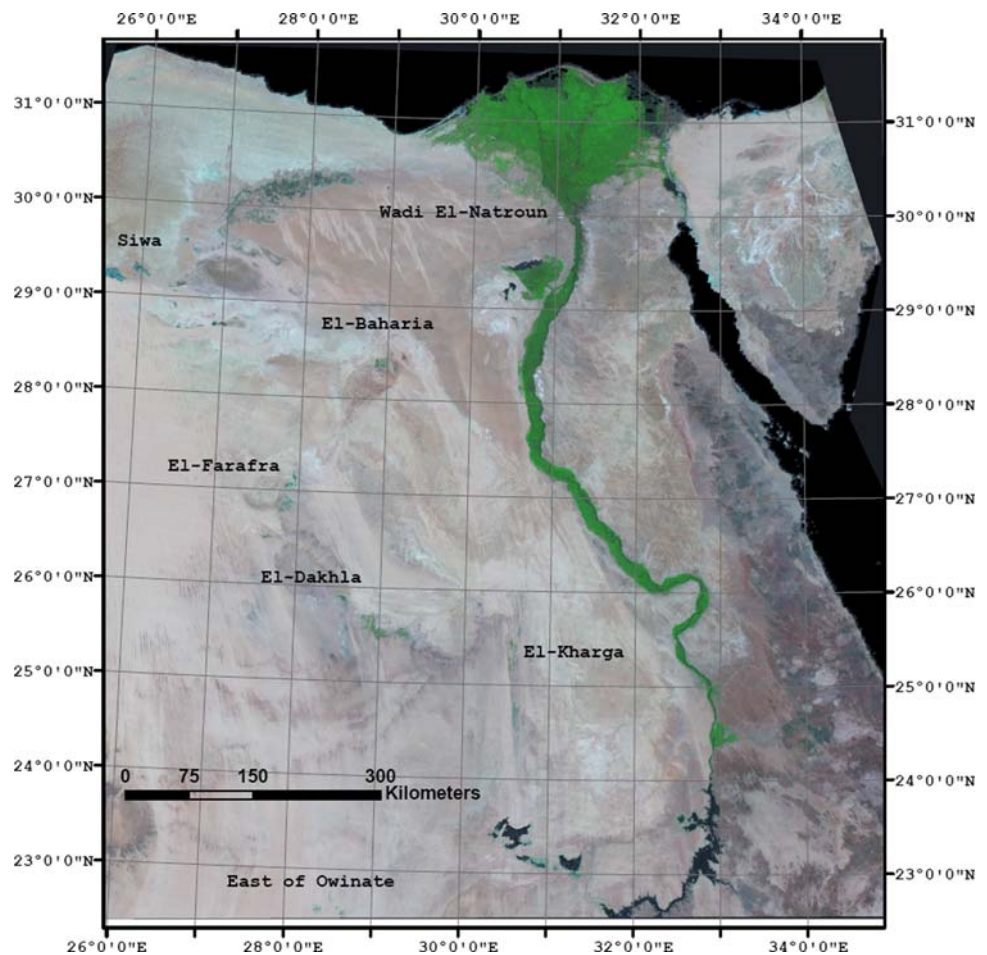
Wind data and sand drift potential calculations

Surface wind data were acquired from the Egyptian Meteorological Authority for seven meteorological stations distributed along the Western Desert of Egypt, from north to south: Wadi El-Natroun; Siwa Oasis; El-Baharia Oasis; El-Farafra Depression, El-Dakhla Oasis; El-Kharga Oasis and East of Owinate region (Fig. 1). The wind data record span 40 years for all meteorological stations (1968–2007) except for the East of Owinate station at the extreme southern part of the desert, which covers 28 years (1980–2007). The wind data come in a standard format and represent the annual average of the percent of hourly occurrence of surface wind measured at 10 m height above ground and are arranged into 12 wind speed classes in 12 directions (Table 1). Since the threshold velocity of moving sand is about 12 knots (6 m/s; Fryberger 1979), all wind speeds below this threshold velocity (below the class 11–16 knots) were excluded from sand drift potential calculations. Sand drift potential refers to the amount of sand moved by the surface wind. The drift potential (DP) is the most important index used for judging wind energy (Lancaster 1995). Sand drift potential is estimated using Fryberger (1979) equation, as follows:

$$DP = V^2(V - V_t) \cdot t$$

where DP refers to the sand drift potential in vector units (VU), V is the average wind speed in knots at 10 m height, t is the percent of wind occurrence in each direction, and V_t is the threshold velocity (12 knots). The term $V^2(V - V_t)$ of the equation is known as the weighting factor in which stronger winds have high weighting factor and weaker winds have low weighting factor. The value of the weighting factor is divided by 100 when the drift potential is represented graphically as sand roses (Fryberger 1979). Table (2) represents an example of calculating the weighting factors from wind data. It is assumed that the surface over which the sediments move consists of dry, loose sand (0.25–0.30 mm diameter) and with sparse

Fig. 1 MODIS mosaic of Egypt showing the locations of the sand dune fields



vegetation cover. The abovementioned equation is applied for each location to estimate the annual sand drift potential in vector units (VU). The value of drift potential in vector unit is translated to the corresponding amount of sand creep as each VU represents 0.07 m^3 of sand moving across 1 m width of land (Fryberger et al. 1984). Annual sand roses were plotted for each location. Wind energy classification was adopted according to Fryberger (1979) as: low-energy wind environment (DP less than 200 VU); intermediate-energy wind environment (DP of 200–399 VU); and high-energy wind environment (DP greater than 400 VU). Fryberger (1979) used the terms resultant drift potential (RDP) and resultant drift direction (RDD) to refer to the magnitude and the trend of the vector results, respectively. The RDP and RDD were calculated by vector analysis for each sand rose to express the net amount of drift and its direction, respectively. The index of the directional variability of surface wind (RDP/DP), which is the ratio of the RDP to the total DP is calculated. Lower RDP/DP values indicate greater directional variability of wind, whereas higher RDP/DP values means that the wind comes from the same direction.

Satellite images and dunes identification

Since the launch of the Landsat satellite series in the early 1970s, a global observation of inaccessible aeolian landforms in arid lands emerged. In this study, seven Landsat Enhanced Thematic Mapper Plus (ETM+) images were utilized to survey and visually interpret the major sand dune fields in the Western Desert of Egypt (Table 3). Each image covers an area of $185 \times 185 \text{ km}$ in six spectral bands at a spatial resolution of 30 m. All images were acquired in the fall and winter seasons of the years 2000 and 2001. Due to the occurrence at the arid belt of the world, the images are clear from clouds. The images were acquired from the Global Land Cover Facility at the University of Maryland, USA (<http://glcf.umiacs.umd.edu/index.shtml>). ArcGIS Software package was used to interpret satellite data. The near infrared (NIR) band (band 4) was the best to discriminate sand dunes from other surface landforms. Each image was displayed at a scale of 1:250,000 and the dune forms at each location were identified according to Breed et al. (1979). In addition, MODIS satellite mosaic of Egypt was compiled

Table 1 Percentage of occurrence and direction of surface wind at the station El-Kharga, from January 1968 to July 2007 (Source: Egypt. Meteorological Authority)

| | 1–3 | 4–6 | 7–10 | 11–16 | 17–21 | 22–27 | 28–33 | 34–40 | 41–47 | 48–55 | 56–63 | >063 | All speeds |
|----------------|------|------|------|-------|-------|-------|-------|-------|-------|-------|-------|------|------------|
| Calm | 0.0 | 0.0 | 0.0 | 0.0 | 0.0 | 0.0 | 0.0 | 0.0 | 0.0 | 0.0 | 0.0 | 0.0 | 0.8 |
| 345–014 | 3.7 | 5.9 | 9.7 | 10.7 | 2.3 | 0.3 | 0.0 | 0.0 | 0.0 | 0.0 | 0.0 | 0.0 | 32.6 |
| 15–44 | 3.0 | 2.9 | 3.0 | 2.0 | 0.2 | 0.0 | 0.0 | 0.0 | 0.0 | 0.0 | 0.0 | 0.0 | 11.2 |
| 45–74 | 1.7 | 0.9 | 0.3 | 0.0 | 0.0 | 0.0 | 0.0 | 0.0 | 0.0 | 0.0 | 0.0 | 0.0 | 2.9 |
| 75–104 | 1.3 | 0.3 | 0.0 | 0.0 | 0.0 | 0.0 | 0.0 | 0.0 | 0.0 | 0.0 | 0.0 | 0.0 | 1.7 |
| 105–134 | 1.3 | 0.3 | 0.0 | 0.0 | 0.0 | 0.0 | 0.0 | 0.0 | 0.0 | 0.0 | 0.0 | 0.0 | 1.6 |
| 135–164 | 0.8 | 0.4 | 0.1 | 0.0 | 0.0 | 0.0 | 0.0 | 0.0 | 0.0 | 0.0 | 0.0 | 0.0 | 1.4 |
| 165–194 | 0.6 | 0.4 | 0.2 | 0.1 | 0.0 | 0.0 | 0.0 | 0.0 | 0.0 | 0.0 | 0.0 | 0.0 | 1.4 |
| 195–224 | 0.6 | 0.2 | 0.1 | 0.0 | 0.0 | 0.0 | 0.0 | 0.0 | 0.0 | 0.0 | 0.0 | 0.0 | 1.0 |
| 225–254 | 1.4 | 0.3 | 0.1 | 0.1 | 0.0 | 0.0 | 0.0 | 0.0 | 0.0 | 0.0 | 0.0 | 0.0 | 1.9 |
| 255–284 | 1.8 | 0.6 | 0.3 | 0.1 | 0.0 | 0.0 | 0.0 | 0.0 | 0.0 | 0.0 | 0.0 | 0.0 | 2.8 |
| 285–314 | 2.8 | 1.6 | 1.3 | 0.6 | 0.0 | 0.0 | 0.0 | 0.0 | 0.0 | 0.0 | 0.0 | 0.0 | 6.4 |
| 315–344 | 7.2 | 7.8 | 10.1 | 8.3 | 0.8 | 0.1 | 0.0 | 0.0 | 0.0 | 0.0 | 0.0 | 0.0 | 34.2 |
| All directions | 26.3 | 21.6 | 25.3 | 22.0 | 3.5 | 0.4 | 0.0 | 0.0 | 0.0 | 0.0 | 0.0 | 0.0 | 100.0 |

Table 2 An example to demonstrate the calculation of weighting factors using Fryberger (1979) equation

| Wind speed category (knots) | Mean wind in category (V) | V^2 | $(V - V_d)$ | Weighting factor $V^2 (V - V_d)/100$ |
|-----------------------------|---------------------------|---------|-------------|--------------------------------------|
| 11–16 | 13.5 | 182.25 | 1.5 | 2.73 |
| 17–21 | 19.0 | 361.00 | 7.0 | 25.27 |
| 22–27 | 24.5 | 600.25 | 12.5 | 75.03 |
| 28–33 | 30.5 | 930.25 | 18.5 | 172.09 |
| 34–40 | 37.0 | 1369.00 | 25.0 | 342.3 |

Table 3 Available satellite images of the studied sand dune fields

| | Location | Path | Row | Date | Sensor |
|---|-----------------|------|-----|-------------------|--------|
| 1 | Wadi El-Natroun | 177 | 39 | 23 December 2001 | ETM+ |
| 2 | Siwa | 180 | 40 | 6 October 2000 | ETM+ |
| 3 | El-Baharia | 177 | 40 | 4 October 2001 | ETM+ |
| 4 | El-Farafra | 178 | 41 | 25 September 2001 | ETM+ |
| 5 | El-Dakhla | 177 | 42 | 4 October 2001 | ETM+ |
| 6 | El-Kharga | 176 | 42 | 10 October 2000 | ETM+ |
| 7 | El-Kharga | 176 | 42 | 29 September 1987 | TM |
| 8 | East of Owinate | 178 | 44 | 11 December 2000 | ETM+ |
| 9 | East of Owinate | 178 | 44 | 27 September 1987 | TM |

from four individual MODIS scenes (H20V5, H20V6, H21V5 and H21V6) acquired in 2005 to show the regional distribution of sand deposits in the Western Desert of Egypt (Fig. 1). The MODIS images (MOD 13 Q1 product) were acquired from the United States Geological Survey (USGS) and were provided in a sinusoidal projection. The pixel size is 231 m, thus they were used

for regional rather than local sand dunes perspective. MODIS images were reprojected to the same projection of the ETM+ images (Universal Transverse Mercator, UTM).

Sand dune migration measurements

Remote sensing has been used successfully in sand dune movement studies (e.g. Yao et al. 2007). Two groups of barchan dunes were selected at El-Kharga and East of Owinate dune fields for measuring dune advance using Landsat satellite images. Fortunately, there were two Landsat images acquired for each location in 1987 and 2000. The images of 1987 are from the Landsat Thematic Mapper (TM) sensor. The two images of 2000 are from the ETM+ sensor (Table 3). In ERDAS Imagine 9.0 Software, the images were displayed at a scale of 1:50,000. The NIR band was chosen to display the sand dunes in each image. Two groups of barchan (crescentic) sand dunes were chosen at both El-Kharga and East of Owinate regions. Sand dune displacement at each location was measured in metres in the two satellite images.

Results and discussion

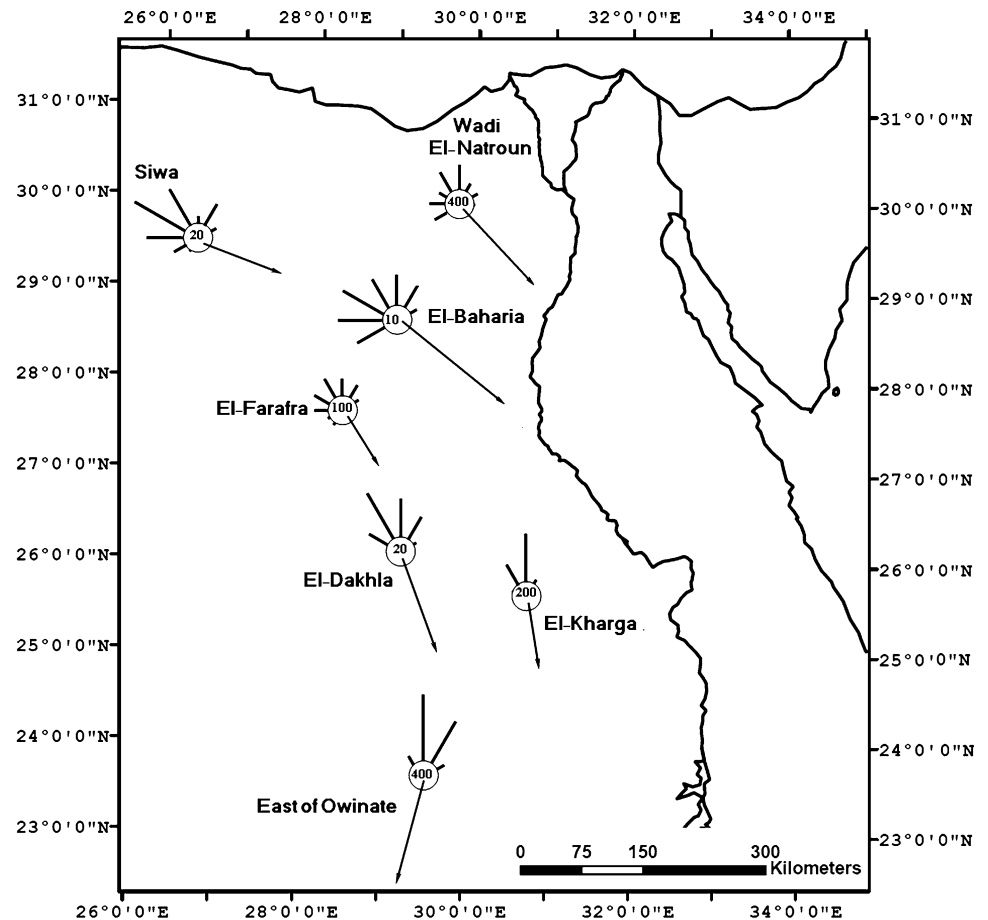
Wind regimes and sand drift potential

Wind data obtained from the seven meteorological stations reveal a considerable variation of strength. Effective wind (>12 knots) is maximal at both the southern and northern edges of the desert. Effective winds blow at 46.7 and 38.1% of time at the East of Owinate region in the

Table 4 The percent of effective wind at each location, the calculated drift potential (DP), the corresponding amount of drift potential in cubic metres per metre width, the resultant drift potential (RDP), the directional variability index (RDP/DP), dominant dune type, the calculated resultant drift direction (RDD), and the actual direction of dunes at each location

| | Effective wind % | DP (VU) | Sand drift (m ³ /m) | RDP (VU) | RDP/DP | Dune type | RDD | Actual direction |
|-----------------|------------------|---------|--------------------------------|----------|--------|------------|-------|------------------|
| Wadi El-Natroun | 38.1 | 440 | 30.8 | 219 | 0.5 | Linear | S43°E | S20°E |
| Siwa | 10.0 | 56 | 3.92 | 18 | 0.32 | Barchanoid | S70°E | S70°E |
| El-Baharia | 7.6 | 27 | 1.89 | 14 | 0.52 | Linear | S51°E | S30°E |
| El-Farafra | 17.8 | 102 | 7.14 | 63 | 0.62 | Linear | S32°E | S25°E |
| El-Dakhla | 8.3 | 31 | 2.17 | 21 | 0.68 | Linear | S20°E | S22°E |
| El-Kharga | 25.9 | 173 | 12.11 | 142 | 0.82 | Barchan | S09°E | S04°E |
| East of Owinate | 46.7 | 571 | 39.97 | 447 | 0.78 | Barchan | S15°W | S20°W |

Fig. 2 Sand roses constructed for the studied locations along the Western Desert. Arrows refer to the resultant drift direction (RDD). The numbers inside each rose represent the reduction or scaling factor

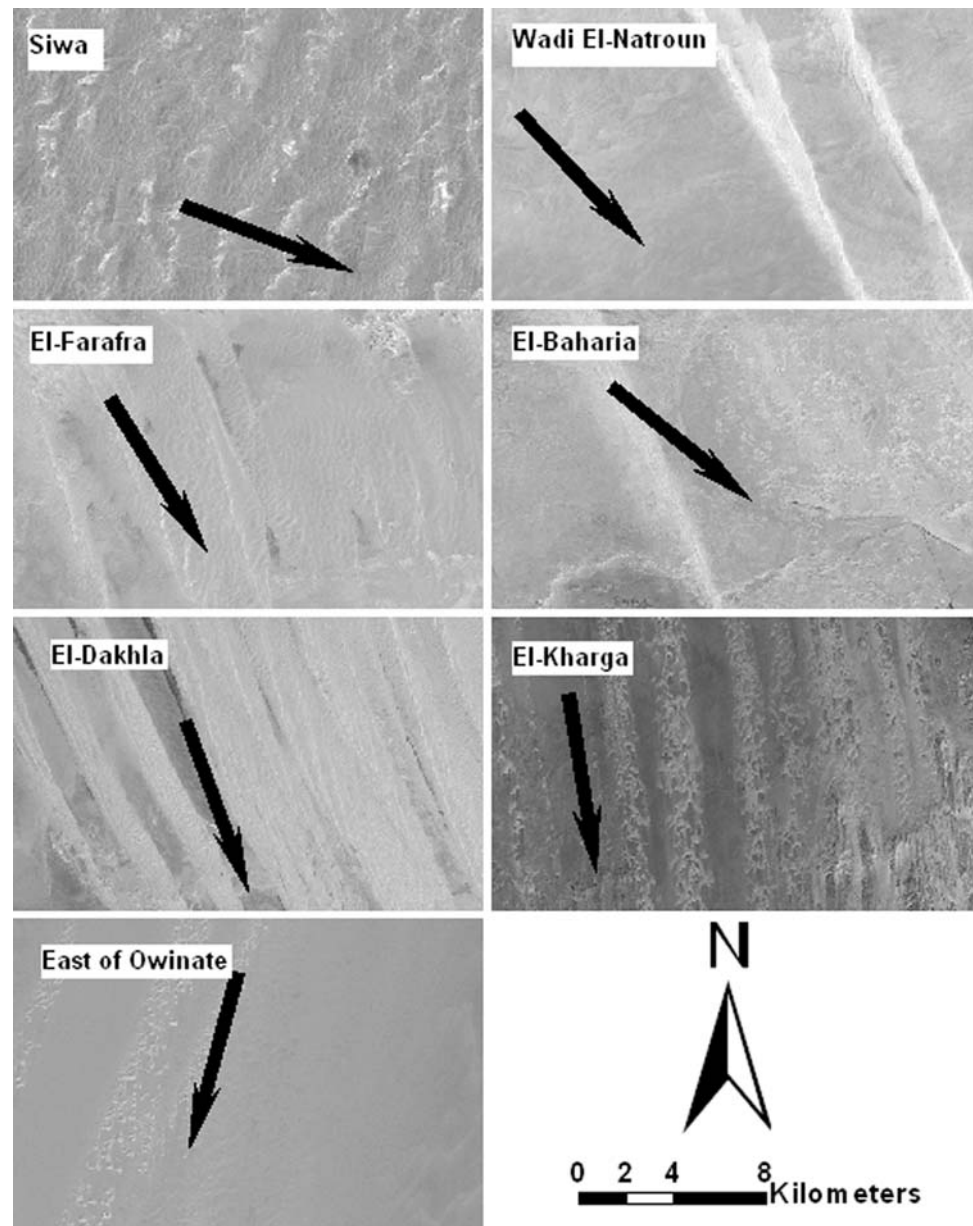


extreme southern part and Wadi El-Natroun in the extreme northeastern part of the desert, respectively. The minimum effective wind is encountered at El-Baharia Oasis at the middle of the desert (7.6% of time). The dominant wind direction at the stations of the northern half of the desert is from the northwest. El-Kharga Depression at the southern half of the desert has dominant winds mostly from the northwest (34.2% of time) and from the north (32.6% of time) directions, whereas at East

of Owinate station at the extreme southern part of the desert, wind blows significantly from the north (42.4% of time) and from the northeast (35.4% of time) directions. This distribution of wind throughout the Western Desert of Egypt indicates a clockwise direction; i.e. northwesterly at the north; northerly at the middle and northeasterly at the south.

Sand drift potential is coincident with both the strength and direction of the effective winds (Table 4). It is

Fig. 3 sand dune forms at the studied locations as observed from Landsat ETM+ images. The *arrow* refers to the direction of the calculated sand drift direction. The sand dunes appear as: transverse at Siwa; linear at Wadi El-Natroun, El-Baharia, El-Farafra and El-Dakhla; and barchan at El-Kharga and East of Owinate



observed that the drift potential is greatest (571 VU) at the extreme southern edge of the desert (East of Owinate). At the northeastern corner (Wadi El-Natroun), it approaches 440 VU. According to Fryberger (1979) classification of wind, both the edges of the desert belong to the high-energy wind environments (>400 VU). RDD is towards the southeast at Wadi El-Natroun and towards southwest at East of Owinate region. All other regions belong to low-energy wind environments (<200 VU). RDD is towards the southeast direction at these regions. The minimum drift potential is encountered at El-Baharia Oasis (7.6 VU). The corresponding amount of sand drifting, in which each VU equals $0.07 \text{ m}^3/\text{m-w}/\text{year}$ of sand (Fryberger et al. 1984), is maximal at East of

Owinate, where about $40 \text{ m}^3/\text{m-w}/\text{year}$ of sand is transported by wind. The least calculated amount is observed at El-Baharia Oasis ($1.89 \text{ m}^3/\text{m-w}/\text{year}$). At Wadi El-Natroun, the amount of sand drift is estimated at about $31 \text{ m}^3/\text{m-w}/\text{year}$. These results reveal that the southern part of the Western Desert is characterized by the maximum sand activity and drifting.

Sand dune forms

Sand dunes as observed from satellite images indicate that linear dunes are the most dominant and widespread throughout the Western Desert. This result conforms with what mentioned by Jordan (1964) that 72% of the Sahara

sand seas were covered by linear dunes. Simple linear dunes are obvious at Wadi El-Natroun, El-Baharia Oasis, El-Farafra and at El-Dakhla Oases (Figs. 1, 2, 3). The dunes in these areas consist of a single narrow dune ridge with straight crest lines. According to Hunter et al. (1983), linear dunes are divided based on the relation between the trend of the dune to the trend of resultant sand-transport direction into longitudinal dunes, which are roughly parallel to the resultant transport direction (within 15° angle), and oblique linear dunes that lie within 15°–75° from the trend of the resultant sand movement. Linear dunes of El-Farafra and El-Dakhla regions (Table 4) belong to the longitudinal type, i.e. the angle between their trend and the resultant drift direction is less than 15°. At Wadi El-Natroun and El-Baharia regions, linear dunes belong to the oblique type, i.e. their trends are aligned at 23° and 21° angles with the RDD of sand, respectively. These variations between the dune direction and the resultant sand drift direction may be attributed to the effect of local topography. Transverse dunes are observed at Siwa, El-Kharga and East of Owinate. According to the classification of Breed et al. (1979) and based on satellite images, these transverse dunes are of the barchanoid ridge type at Siwa and of the simple barchans at both El-Kharga and East of Owinate. At Siwa, which borders the northern periphery of the Great Sand Sea and the sand supply is abundant, the slip faces of the dunes are observed facing the southeast direction (Fig. 3). Although the dunes at Siwa are aligned transverse to the RDD, directional variability index ($RDP/DP = 0.32$) reveals that wind blows from multiple wind directions. At both El-Kharga and East of Owinate regions, simple barchans form chains extending parallel to the RDD (Fig. 3). At El-Kharga Depression, the sand supply is limited due to the presence of the northern escarpment of the depression, which hampers much sand from reaching the depression floor. Limited supply of sand is funnelled forming these barchan sand dunes (Fig. 3). On the other hand, barchans at East of Owinate were formed due to the distance from the sand supply, i.e. the Great Sand Sea, where the sand supply is also limited.

Correlating wind regimes prevailing throughout the Western Desert with the dune forms indicates that linear dunes are generally associated with bimodal wind regime (lower RDP/PD values), which means that winds blow from many directions. These results agree with the hypothesis of Fryberger (1979). The value of the directional variability index, RDP/DP , is 0.50 at Wadi El-Natroun, 0.52 at El-Baharia Oasis, 0.62 at El-Farafra Oasis and 0.68 at El-Dakhla Oasis. On the other hand, barchan dunes are associated with unimodal wind regime (higher RDP/PD values) indicating lower variability of wind direction. The RDP/DP values approach 0.82 at El-Kharga Depression and 0.78 at East of Owinate region. The only exception is

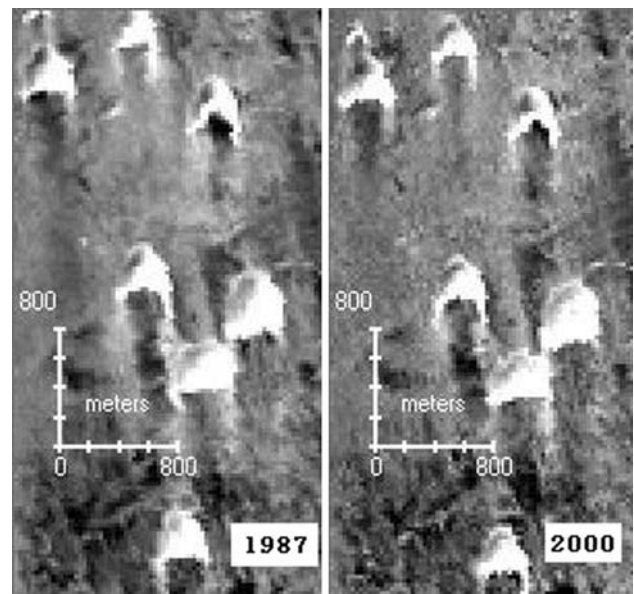


Fig. 4 Sand dune movements at El-Kharga Depression. Note the displacement in the two satellite images of 1987 and 2000

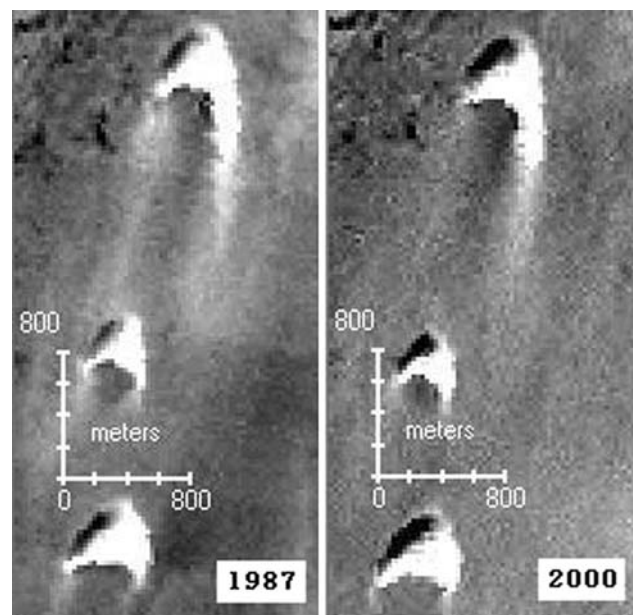


Fig. 5 Sand dune movements at East of Owinate. Note the displacement in the two satellite images of 1987 and 2000

observed at Siwa Oasis, where the prevailing dune type is the transverse ridge and the associated wind has a bimodal regime ($RDP/DP = 0.32$).

Sand dunes movement

Barchan (crescentic) dunes were observed in satellite images only at El-Kharga and East of Owinate regions. At these locations, dune movements reflect the energy of

Fig. 6 Sand encroachment upon infrastructures at El-Baharia Oasis



surface wind. At El-Kharga, five dunes were examined from satellite data. The amount of dune advance between 1987 and 2000 ranges from 55 m to 128 m for the selected dunes (Fig. 4). The average dune advance was 98 m with an annual rate of 7.5 m/year. This result is comparable to some previous studies (e.g. Tag El-Din 1986 and Embaby 1986). At East of Owinate, the dunes examined from satellite data showed that the movement between 1987 and 2000 ranges from 84 to 145 m (Fig. 5). The average dune movement was 118.5 m with an annual rate of 9.1 m/year. The results of dune advance rate at these locations significantly correlate with the energy of surface wind at these locations in terms of the amount of annual sand drift potential. In other words, the drift potential calculated for El-Kharga and East of Owinate is translated to be equal $12 \text{ m}^3/\text{m-w}/\text{year}$ of sand at the former and $40 \text{ m}^3/\text{m-w}/\text{year}$ of sand at the latter.

Sand encroachment hazards

Sand encroachment means the accumulation of aeolian sediment upon man-made constructions due to their interference with the sand-driven wind regimes (Khalaf and Al-Ajmi 1993). The moving sand sometimes creates serious hazards to new roads, settlements and agricultural lands. This problem is triggered by the extreme arid conditions in this desert. From field investigations, sand encroachment problems were observed mainly in the oases of the desert (Fig. 6). However, it was reported that the dunes of the Western Desert of Egypt encroach on the fertile land west of the Nile Valley (Abu El-Ennan et al. 1990). Moreover, sand encroachment problems and moving dunes represent significant threats to the newly reclaimed lands in the South Valley Development Project at the southern part of the desert. In many reaches of this project, irrigation water is transported by pipes rather than open canals in order to avoid drifting sand and evaporation. Beside

sand movement, dust storms are a frequent phenomenon in this vast desert. During winter and spring, huge quantities of dust are transported by wind, affecting air quality. The dust originating from the Sahara desert constitutes a major source of aeolian dust to the atmosphere (Mattsson and Nihlen 1994). This dust is carried over thousands of kilometres and sometimes reaches the Americas, Europe and Near East (Goudie 2002).

Conclusions

This paper provides an analysis of wind regimes prevailing throughout the Western Desert of Egypt with the associated dune forms. The trend of sand movement is observed following a clockwise pattern. Results suggest that the variability of wind strength and direction is responsible for the occurrence of different forms of sand dune. There is some kind of deviation between the trend of sand dunes and the net trend of the sand-driving wind. This may be partially attributed to the local topographic variations, since the majority of the meteorological stations are situated within the semi-closed depressions in the desert, while the sand dunes are at higher levels. The source of sand in these dunes deserves much attention. Although some studies attribute the source of sand to the previous fluvial sources, mineralogy studies are needed to support this hypothesis. The study also proves that Landsat data provide invaluable information about sand dunes advance measurements in remote and inaccessible arid desert areas.

References

- Abu El-Ennan SM, Dalsted KJ, Salem MZ (1990) Dune encroachment on the cultivated land in Egypt. *Desert Control Bull* 18:1–5

- Bagnold R (1941) *The physics of blown sand and desert dunes*. Methuen, London, p 265
- Breed CS, Fryberger SC, Andrews S, McCauley C, Lennartz F, Gebel D, Hortman K (1979) Regional studies of sand seas using Landsat (ERTS) imagery. In: McKee ED (ed) *A study of global sand seas: Geological Survey Professional Paper, 1052*. United States Geological Survey, Washington DC, pp 305–397
- Brookes IA (2003) Geomorphic indicators of Holocene winds in Egypt's Western Desert. *Geomorphology* 56:155–166
- El-Baz F (1986) Monitoring the sand-moving desert winds. In: El-Baz F, Hassan M (eds) *Physics of desertification*. Martinus Nijhoff, The Netherlands, pp 141–158
- El-Baz F, Maxwell T (1982) Desert landforms of southwest Egypt: a basis for comparison with Mars. NASA, Scientific and Technical Information Branch, Washington DC
- El-Baz F, Maingue M, Robinson C (2000) Fluvio-aeolian dynamics in the north-eastern Sahara: the relationship between fluvial/aeolian systems and ground-water concentration. *J Arid Environ* 44:173–183
- Embaby NS (1986) Dune movement in the Kharga and Dakhla Oases Depressions, Western Desert, Egypt. *Bull Soc Geog D'Egypt* 59–60, 35–70
- Fryberger SG (1979) Dune forms and wind regime. In: McKee ED (ed) *A study of global sand seas, Geological Survey Professional Paper, 1052*. United States Geological Survey, Washington DC, pp 137–169
- Fryberger SG, Al-Sari AM, Clisham TJ, Rizvi SR, Al-Hinai KG (1984) Wind sedimentation in the Jafurah Sand Sea, Saudi Arabia. *Sedimentology* 31:413–431
- Ghoneim E, El-Baz F (2007) The application of radar topographic data to mapping of a mega-paleodrainage in the Eastern Sahara. *J Arid Environ* 69:658–675
- Gifford AW, Warner DM, El-Baz F (1979) Orbital observation of sand distribution in the Western Desert of Egypt. In: El-Baz F, Warner D (eds) *Apollo-Soyuz Test Project summary science report, vol II*. National Aeronautics and Space Administration, Washington DC
- Goudie AS (2002) *Great warm desert of the world: landscapes and evolution*. Oxford University Press, New York, p 444
- Hunter R, Richmond B, Alpha T (1983) Storm-controlled oblique dunes of the Oregon coast. *Geol Soc Am Bull* 94:1450–1465
- Jordan WM (1964) Prevalence of sand dune types in the Sahara desert. *Geological Society of America, Special Paper* 82, pp 104–105
- Khalaf FI, Al-Ajmi D (1993) Aeolian processes and sand encroachment problems in Kuwait. *Geomorphology* 6:111–134
- Lancaster N (1995) *Geomorphology of desert dunes*. Rutledge, London, pp 1–7
- Le Houerou HN (1997) Climate, flora and fauna changes in the Sahara over the past 500 million years. *J Arid Environ* 37:619–647
- Mattsson J, Nihlen T (1994) The transport of Saharan dust to southern Europe: a scenario. *J Arid Environ* 32:111–119
- Tag El-Din SS (1986) Some aspects of sand stabilization in Egypt. In: El-Baz F, Hassan MH (eds) *Physics of desertification*. Martinus Nijhoff Publishers, The Netherlands, pp 118–126
- Vogg R, Wehmeier E (1985) Arid environment and land classification of the South Valley, Toshka (Western Desert, Egypt). *J Arid Environ* 9:1–12
- Yao ZY, Wang T, Han ZW, Zhang WM, Zhao AG (2007) Migration of sand dunes on the northern Alxa Plateau, Inner Mongolia, China. *J Arid Environ* 70:80–93